



A high efficient assembly technique for large PEMFC stacks

Part I. Theory

P. Lin, P. Zhou, C.W. Wu*

State Key Lab of Structural Analysis for Industrial Equipment, Faculty of Vehicle Engineering and Mechanics, Dalian University of Technology, Dalian 116024, China

ARTICLE INFO

Article history:

Received 10 March 2009
Received in revised form 25 April 2009
Accepted 27 April 2009
Available online 3 May 2009

Keywords:

Fuel cell
Proton exchange membrane
Clamping load
Assembly technique

ABSTRACT

A high efficient assembly technique for large proton exchange membrane fuel cell (PEMFC) stacks is proposed to obtain the optimal clamping load. The stack system is considered as a mechanical equivalent stiffness model consisting of numerous elastic elements (springs) in either series or parallel connections. We first propose an equivalent stiffness model for a single PEM fuel cell, and then develop an equivalent stiffness model for a large PEMFC stack. Based on the equivalent stiffness model, we discuss the effects of the structural parameters and temperature on the internal stress of the components and the contact resistance at the contact interfaces, and show how to determine the assembly parameters of a large fuel cell stack using the equivalent stiffness model. Finally, a three-dimensional finite element analysis (FEA) for a single PEMFC is compared with what the equivalent stiffness model predicts. It is found that the presented model gives very good prediction accuracy for the component stiffness and the clamping load.

© 2009 Elsevier B.V. All rights reserved.

1. Introduction

Fuel cell technology has been achieved a great jumping development during the past decade. Especially, the PEMFC offers a possible substitute for the combustion engine owing to its high power efficiency and low level of pollution. Although most of the studies on fuel cells in laboratories are focused on the performance of a single cell [1–11], they are very helpful for us to understand the basic principle of the fuel cell and to enhance the fuel cell performance. However, for a large fuel cell stack, the assembly technique is one of the key techniques to ensure the stack having a long lifetime and high reliability. Previous studies have shown that the clamping load (pressure) in the assembly of a single cell plays an important role in optimizing the performance of the fuel cell [1–7]. However, there has been no detailed study for the assembly of a large fuel cell stack since the optimal clamping load is more difficult to determine than for a single cell due to the complex system structure and working environment.

The clamping load of a large fuel cell stack affects the lifetime and performance of the stack system in several ways. Too large a clamping load may cause some components in the stack to produce a stress high enough to give rise to plastic deformation even cracks [12], while an unreasonable small clamping load may produce a high contact electrical resistance at the interface of the gas diffu-

sion layer (GDL) and the bipolar plate (BPP) [1–3], and also may cause leakage of water or fuel in the seal interfaces [13]. It should also be pointed out that even though a reasonable initial clamping load had been given in the assembly process at room temperature, either the contact electrical resistance or the seal interface pressure or the structure stress may be out of the allowed region of the design due to the thermal deformations of the fuel cell components under working conditions. To overcome those problems occurred during the stack running, the stiffness of both the clamping components and the clamped components have to be optimized. For example, in the bolt assembling (a traditional assembly technique), both the stiffness and the strength of the bolts should be first optimized. However, the following problems are still the challenging techniques in the structure design of a large fuel cell stack: (a) how to determine the clamping load of the stack; (b) how to design the stiffness and strength of the clamped components; (c) how to design the geometry and stiffness of the sealants; (d) how to design the bipolar plates, including the structural shape and size, etc.

Strictly speaking, the design of a reasonable clamping load and an optimal stiffness of the related components for a large fuel cell stack needs a detailed finite element analysis (FEA) for the whole system. Nowadays, complex FEA can be obtained by virtue of highly developed computer technology and constantly improved software codes. However, it is difficult to form an ideal FEA model of the large fuel cell stack due to its multi-scale structural characteristics. For example, in order to guarantee the reasonable calculation accuracy, for the membrane electrode assembly (MEA), the size of the elements should be on the order of micrometers [1–3]; for

* Corresponding author. Tel.: +86 411 84706353; fax: +86 411 84706353.
E-mail address: cwwu@dlut.edu.cn (C.W. Wu).

Nomenclature

k	equivalent stiffness of a component (N mm^{-1})
F	load applied on the component (N)
E	elastic modulus (N mm^{-2})
A	cross section area (mm^2)
L	length of the component along the clamping load direction (mm)
C	number of the clamping bolts
N	number of the flow channels on one side of the bipolar plate
M	number of the cells of a large stack
Z^F	clamping deformation (mm)
Z^T	free thermal deformation (mm)
ΔT	temperature changes ($^{\circ}\text{C}$)

Greek letters

α	coefficient of heat expansion ($^{\circ}\text{C}^{-1}$)
----------	---

the interface between the GDL and the ribs of the BPP, the contact element size should be on the order of $10\ \mu\text{m}$; for the bipolar plate, the element size should range between $10\ \mu\text{m}$ and $100\ \mu\text{m}$; however, for the end plates (EP) and the assembling bolts, the element size may range between $100\ \mu\text{m}$ and $1\ \text{cm}$. Thus, the FEA for a large fuel cell stack is a multi-scale nonlinear contact analysis coupled with thermal stress analysis, a really hard topic in the computational mechanics. The number of the total elements may be on the order of several millions even larger. No report has been found so far for such a huge computation for fuel cell structure analysis.

In this paper, we present a high efficient assembly technique for the large PEMFC stacks. The basic idea of the technique is first to assume the stack system consisting of a large number of elastic elements (springs) in either series or parallel connections. For each spring, the stiffness coefficient can be obtained using material mechanics analysis for the simple period structures or using FEA for the complex structures. Then a system analysis technique is used to give the optimal design for each structure component in the stack.

2. Basic model descriptions

Stiffness of a solid body is the resistance offered by an elastic body to deformation. Its value depends on the material property, the structure shape and size, and the boundary conditions of the solid body [14]. As shown in Fig. 1, for an elastic bar under tension or compression, the axial stiffness is:

$$k = \frac{EA}{L} \quad (1)$$

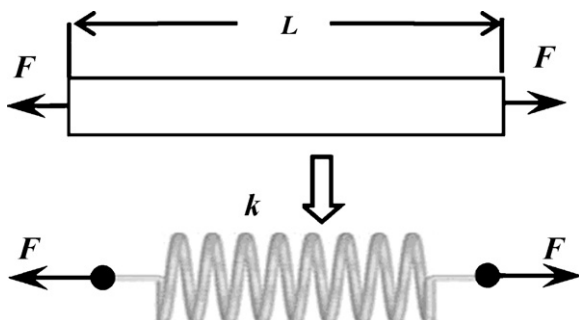


Fig. 1. Schematic of the axial equivalent stiffness of an elastic element.

where k is usually called the equivalent stiffness [15], E is the elastic modulus, A is the cross section area, L is the length of the bar along the axial direction. As for a complex structure, the equivalent stiffness cannot be simply obtained by Eq. (1). A traditional method is to simplify the structure as an equivalent model consisting of elastic elements (usually springs) in parallel or series connections, and then the deformation of the structure under a load can be obtained through this equivalent model. In this paper, the most we care about is the mechanical behavior of the fuel cell stack along the direction of the clamping load. In the same way, the whole fuel cell stack can be divided into several basic components whose stiffness can be calculated by Eq. (1) according to the load bearing characteristics of the structures along the direction of the clamping load. In order to make the model building process more comprehensive, only a single cell is studied in the first step, the whole stack model can be obtained via cyclically assembling the single cells. Thus the relation of the deformation and the clamping load can be obtained using this equivalent stiffness model.

2.1. Basic assumptions

Proper assumptions are needed before building the equivalent stiffness model. For simplification and theory analysis strictness, the following assumptions are stated:

- (1) The end-plates are treated as rigid body and have an enough high mechanical strength [16]. Although an ideal rigid end-plate is difficult to obtain in practice, an end-plate with a suitable design can be considered as rigid one approximately.
- (2) Each clamping bolt bears the same clamping load and gives the same elongation during assembly.

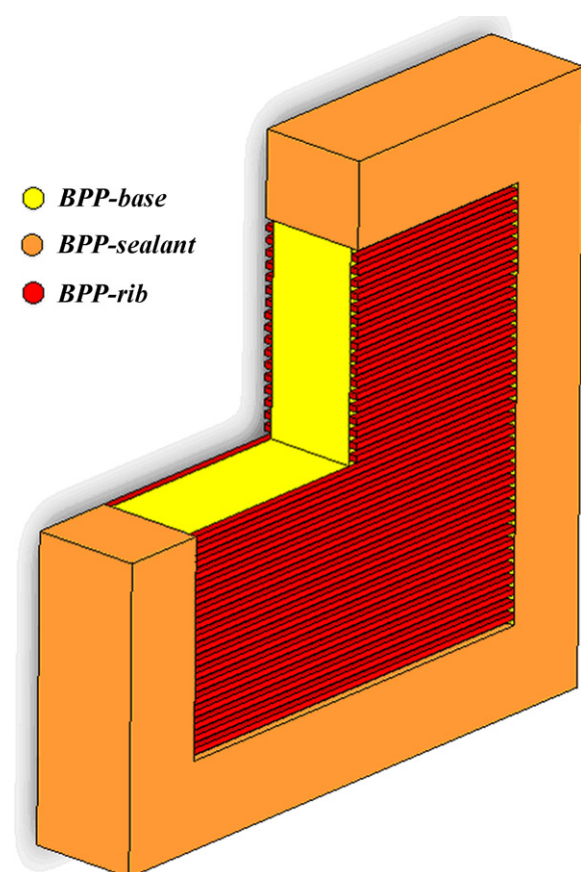
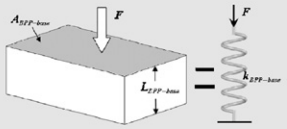
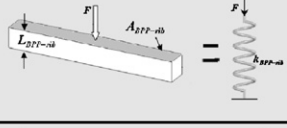
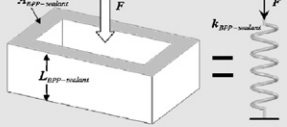
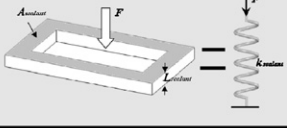
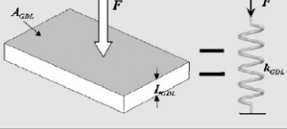
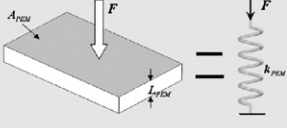


Fig. 2. Schematic of the three regions of the bipolar plate.

Table 1
Stiffness and thermal expansion equations of the basic components.

Component	Schematic	Equivalent Stiffness	Thermal Expansion
BPP-base		$\frac{E_{BPP-base} A_{BPP-base}}{L_{BPP-base}}$	$\alpha_{BPP-base} \Delta T_{BPP-base} L_{BPP-base}$
BPP-rib		$\frac{E_{BPP-rib} A_{BPP-rib}}{L_{BPP-rib}}$	$\alpha_{BPP-rib} \Delta T_{BPP-rib} L_{BPP-rib}$
BPP-sealant		$\frac{E_{BPP-sealant} A_{BPP-sealant}}{L_{BPP-sealant}}$	$\alpha_{BPP-sealant} \Delta T_{BPP-sealant} L_{BPP-sealant}$
sealant		$\frac{E_{sealant} A_{sealant}}{L_{sealant}}$	$\alpha_{sealant} \Delta T_{sealant} L_{sealant}$
GDL		$\frac{E_{GDL} A_{GDL}}{L_{GDL}}$	$\alpha_{GDL} \Delta T_{GDL} L_{GDL}$
PEM		$\frac{E_{PEM} A_{PEM}}{L_{PEM}}$	$\alpha_{PEM} \Delta T_{PEM} L_{PEM}$

- (3) The bipolar plate has N parallel flow channels, while the number of the bipolar plate ribs is $(N - 1)$.
- (4) As shown in Fig. 2, the bipolar plate is divided into three regions: the BPP-sealant, the BPP-rib and the BPP-base.
- (5) MEA is considered as the sandwich structure: GDL + PEM (proton exchange membrane) + GDL [17].
- (6) The coolant plate's stiffness is mixed together with the bipolar plate as a single bipolar plate.
- (7) It is assumed that there are no gaps at the connection interfaces of the fuel cell stack before assembly, i.e., all the MEA and sealants have the same thickness.
- (8) The assembly process is accomplished at room temperature.

In addition, in the following analysis, the model components listed in Table 1 are called the basic components, whose equivalent stiffness can be calculated using equations given in Table 1.

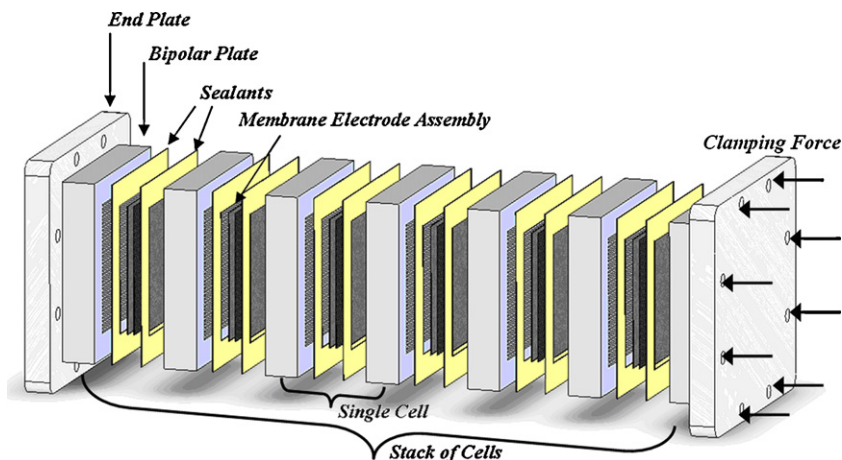


Fig. 3. Schematic of the PEM fuel cell stack hardware.

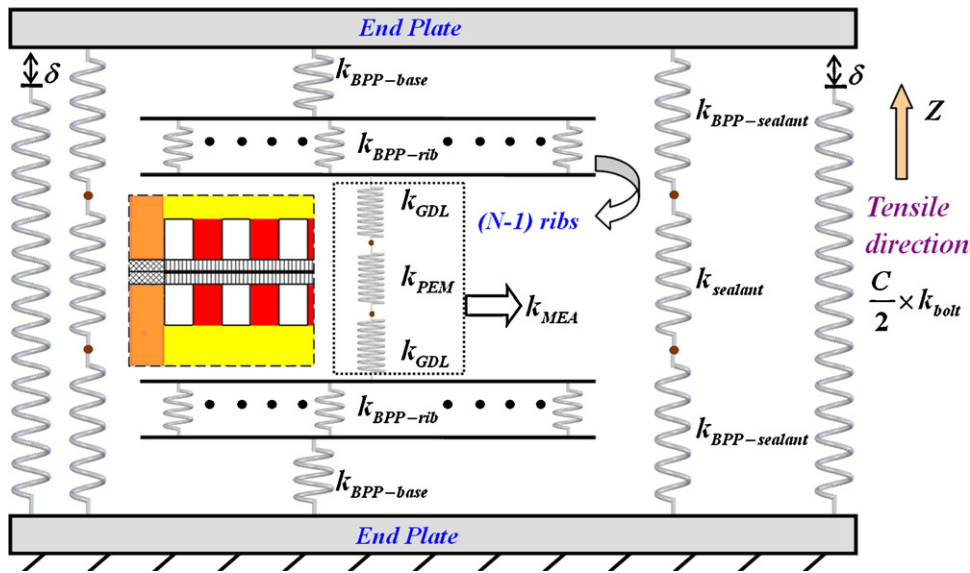


Fig. 4. Schematic of the equivalent stiffness model of the single cell (the dimensions of the springs do not represent the magnitude of stiffness).

The components consisting of the basic components are called the assembled components.

2.2. Equivalent stiffness model of a single PEMFC

As Fig. 3 depicts, a single PEMFC consists of three types of components: a membrane electrode assembly, two bipolar plates and the sealants [17]. They are all included in the following equivalent stiffness model of the single cell.

From the view perpendicular to the flow channels, we have a mechanical equivalent stiffness model of the single cell as shown in Fig. 4, where δ equals the thread pitch times the pretightening cycles of the nuts, and the arrow Z represents the positive direction of the vectors such as displacement or load. The stiffness of each spring in the model equals the equivalent stiffness of the basic component or the assembled component.

Based on assumption (2), we can make further simplification for the system as shown in Fig. 5. This model is a pure mathematical model without any structural characteristics, the guide rails will constrain the rotation of the upper end-plate caused by the unbalanced stiffness distribution. Any way, the displacement along the clamping direction is completely equivalent with the model as shown in Fig. 4.

Subsequently, the equivalent stiffness model can be finally simplified by combining the stiffness of the BPP-sealant and the sealant (basic components) in series as the assembled component: external-cell, and combining the stiffness of the BPP-base and cell-core in series as the assembled component: internal-cell. After those simplifications, the system of one single cell can be simplified as what is shown in Fig. 6. It consists of two end-plates, C clamping bolts, the internal-cell and the external-cell (see Fig. 6).

Based on the model shown in Fig. 6, the equivalent stiffness of a PEM single cell is given:

$$k_{\text{single-cell}} = k_{\text{internal-cell}} + k_{\text{external-cell}} \tag{2}$$

where k is the equivalent stiffness corresponding to the component as indicated in the subscript (similarly hereinafter). For the internal-cell, an assembled component, the equivalent stiffness can be calculated as:

$$k_{\text{internal-cell}} = \frac{1}{2/k_{\text{BPP-base}} + 1/k_{\text{cell-core}}} = \frac{k_{\text{BPP-base}}k_{\text{cell-core}}}{k_{\text{BPP-base}} + 2k_{\text{cell-core}}} \tag{3}$$

where the equivalent stiffness of the assembled component cell-core (see Fig. 5) is:

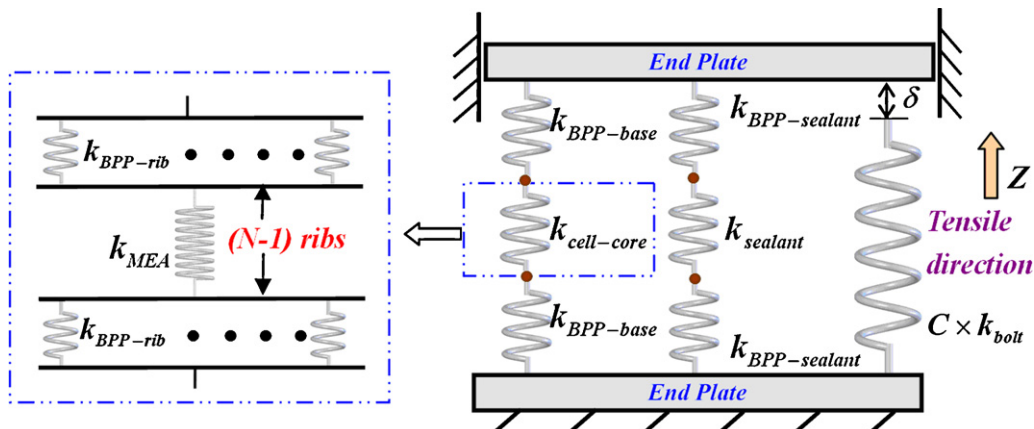


Fig. 5. Schematic of the simplified equivalent stiffness model of the single cell.

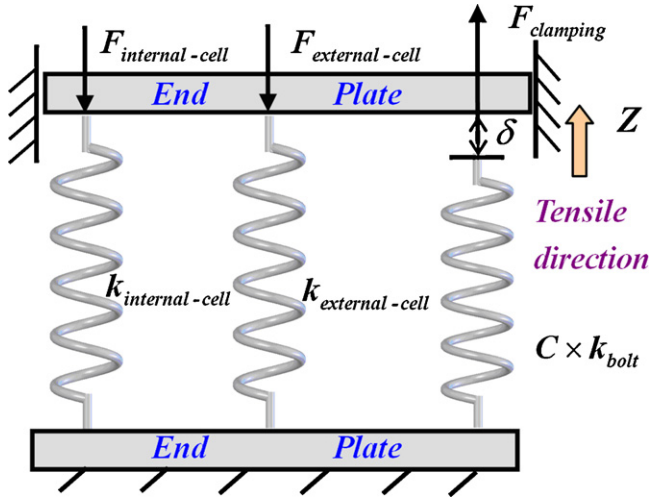


Fig. 6. Schematic of the final equivalent stiffness model of the single cell.

$$k_{\text{cell-core}} = \frac{1}{2 / \sum_{i=1}^{n-1} k_{\text{BPP-rib}}^{(i)} + 1 / k_{\text{MEA}}} = \frac{\left(\sum_{i=1}^{n-1} k_{\text{BPP-rib}}^{(i)} \right) k_{\text{MEA}}}{\left(\sum_{i=1}^{n-1} k_{\text{BPP-rib}}^{(i)} \right) + 2k_{\text{MEA}}} \quad (4)$$

where the superscript *i* represents the number of the ribs. The equivalent stiffness of the MEA is:

$$k_{\text{MEA}} = \frac{1}{2 / k_{\text{GDL}} + 1 / k_{\text{PEM}}} = \frac{k_{\text{GDL}} k_{\text{PEM}}}{k_{\text{GDL}} + 2k_{\text{PEM}}} \quad (5)$$

In the same way, for the assembled component external-cell, the equivalent stiffness can be calculated as follows:

$$k_{\text{external-cell}} = \frac{1}{2 / k_{\text{BPP-sealant}} + 1 / k_{\text{sealant}}} = \frac{k_{\text{BPP-sealant}} k_{\text{sealant}}}{k_{\text{BPP-sealant}} + 2k_{\text{sealant}}} \quad (6)$$

Equivalent stiffness of the basic components can be calculated using the equations given in Table 1. Based on the conditions of compatible displacement and static load equilibrium in Z direction (clamping direction), the structural load equilibrium equation can be written as follows:

$$Ck_{\text{bolt}}(\delta + Z_{\text{single-cell}}^F) + k_{\text{single-cell}}Z_{\text{single-cell}}^F = 0 \quad (7)$$

where the deformation of the whole single cell under the clamping load is:

$$Z_{\text{single-cell}}^F = -\frac{Ck_{\text{bolt}}}{Ck_{\text{bolt}} + k_{\text{single-cell}}} \delta \quad (8)$$

where $Z_{\text{single-cell}}^F$ is a negative number indicating the structures are under compression since δ is positive for bolt stretching. Then the clamping loads applied on the single cell are:

$$\begin{aligned} F_{\text{internal-cell}} &= k_{\text{internal-cell}} Z_{\text{single-cell}}^F \\ &= -\frac{Ck_{\text{bolt}} k_{\text{internal-cell}}}{Ck_{\text{bolt}} + k_{\text{internal-cell}} + k_{\text{external-cell}}} \delta \end{aligned} \quad (9)$$

$$\begin{aligned} F_{\text{external-cell}} &= k_{\text{external-cell}} Z_{\text{single-cell}}^F \\ &= -\frac{Ck_{\text{bolt}} k_{\text{external-cell}}}{Ck_{\text{bolt}} + k_{\text{internal-cell}} + k_{\text{external-cell}}} \delta \end{aligned} \quad (10)$$

The total clamping load applied on the single cell is the sum of $F_{\text{internal-cell}}$ and $F_{\text{external-cell}}$, which equals the load applied on the clamping bolts (see Fig. 6):

$$F_{\text{clamping}} = F_{\text{internal-cell}} + F_{\text{external-cell}} \quad (11)$$

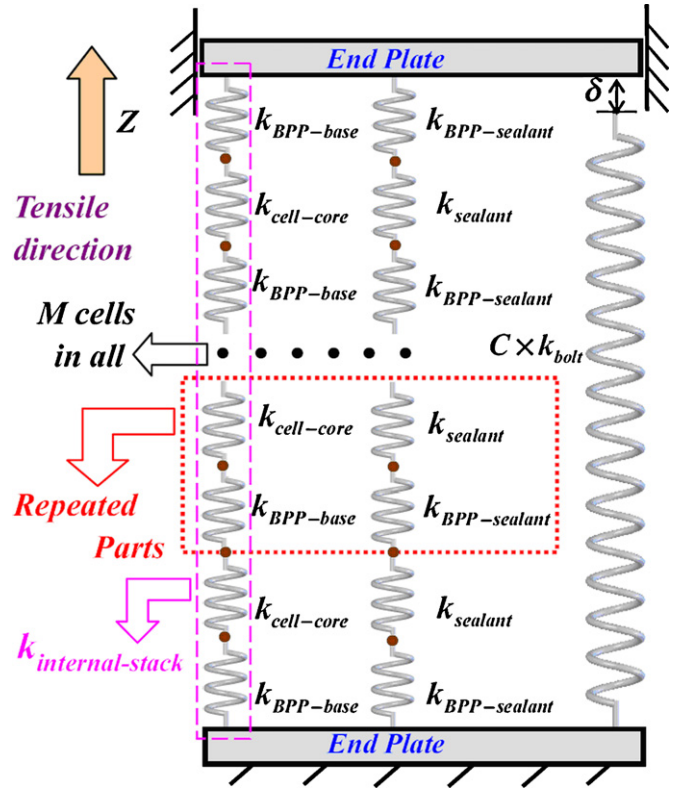


Fig. 7. Schematic of the equivalent stiffness model of the PEM stack.

2.3. Equivalent clamping stiffness model of a PEMFC stack

The PEMFC stack is comprised of numerous cells connected via bipolar plates as is shown in Fig. 3. For this cyclic cell characteristic, stiffness of the whole stack can be obtained by combining the single PEMFC equivalent model in sequence. Fig. 7 depicts the equivalent clamping stiffness model of a PEMFC stack. Therefore, the equivalent stiffness model of the stack can be simplified as the similar model shown in Fig. 6. But here it is composed of the following components: two end plates, C clamping bolts, the internal-stack and the external-stack (see Fig. 7). Now the stack stiffness can be written:

$$k_{\text{stack}} = k_{\text{internal-stack}} + k_{\text{external-stack}} \quad (12)$$

where the stiffness of the internal-stack and the external-stack can be calculated as follows:

$$k_{\text{internal-stack}} = \frac{1}{\sum_{i=1}^{M+1} (1 / k_{\text{BPP-base}}^{(i)}) + \sum_{j=1}^M (1 / k_{\text{cell-core}}^{(j)})} \quad (13)$$

$$k_{\text{external-stack}} = \frac{1}{\sum_{i=1}^{M+1} (1 / k_{\text{BPP-sealant}}^{(i)}) + \sum_{j=1}^M (1 / k_{\text{sealant}}^{(j)})} \quad (14)$$

In Eqs. (12) and (13) the superscript *i* represents the *i*th bipolar plate while *j* represents the *j*th cell. Stiffness of the cell-core can be obtained using Eq. (4). Based on the conditions of compatible displacement and static load equilibrium, the deformation of the whole stack under the clamping load is:

$$Z_{\text{stack}}^F = -\frac{Ck_{\text{bolt}}}{Ck_{\text{bolt}} + k_{\text{stack}}} \delta \quad (15)$$

Also the clamping loads applied on the stack are:

$$\begin{aligned} F_{\text{internal-stack}} &= k_{\text{internal-stack}} Z_{\text{stack}}^F \\ &= -\frac{Ck_{\text{bolt}}k_{\text{internal-stack}}}{Ck_{\text{bolt}} + k_{\text{internal-stack}} + k_{\text{external-stack}}} \delta \end{aligned} \quad (16)$$

$$\begin{aligned} F_{\text{external-stack}} &= k_{\text{external-stack}} Z_{\text{stack}}^F \\ &= -\frac{Ck_{\text{bolt}}k_{\text{external-stack}}}{Ck_{\text{bolt}} + k_{\text{internal-stack}} + k_{\text{external-stack}}} \delta \end{aligned} \quad (17)$$

The total clamping load applied on the stack is the sum of $F_{\text{internal-stack}}$ and $F_{\text{external-stack}}$, which equals the load applied on the clamping bolts:

$$F_{\text{clamping}} = F_{\text{internal-stack}} + F_{\text{external-stack}} \quad (18)$$

2.4. Amendments to the equivalent stiffness model of PEMFC stack

What is discussed above is based on the assumption that there is no gap before assembling at either the interface between the bipolar plate and the MEA or the interface between the bipolar plate and the sealant. This is only an ideal case. In practice, there are usually small gaps before assembling at one of the interfaces mentioned above. We will discuss this general case in Section 2.4.1.

The clamping process is usually carried out at room temperature. However, the modern PEM fuel cell stack usually operates at temperature below 80 °C [18]. All the components will produce thermal stress and deformation under such a temperature. We will also discuss the temperature effect in Section 2.4.2.

2.4.1. Unequal thickness of the MEA and the sealant before assembly

In the case of unequal thickness of the MEA and the sealant before assembly, the bipolar plate will first contact with either the sealant or the GDL. It is assumed that all the cells have the same gap, Z_{initial}^F , defined as below:

$$Z_{\text{initial}}^F = L_{\text{MEA}} - L_{\text{sealant}} \quad (19)$$

where L_{MEA} and L_{sealant} are the thickness of the MEA and the sealant, respectively. When Z_{initial}^F is positive, the gap occurs at the interface of the sealant and the bipolar plate; but when Z_{initial}^F is negative, the gap occurs at the interface of the MEA and the bipolar plate.

Here the total pretightening displacement of the clamping bolts is:

$$\delta_{\text{total}} = \delta_{\text{initial}} + \delta_{\text{fasten}} \quad (20)$$

where δ_{initial} is the pretightening displacement occurring before the gap vanishes at the initial stage of the assembly, δ_{fasten} is the design displacement variable of the clamping bolts after gaps vanish.

In the case of $L_{\text{MEA}} > L_{\text{sealant}}$, we have (see Fig. 8a):

$$\delta_{\text{initial}} = \frac{MZ_{\text{initial}}^F(Ck_{\text{bolt}} + k_{\text{internal-stack}})}{Ck_{\text{bolt}}} \quad (21)$$

where M is number of the cells of a large stack and C is the number of the bolts. With Eq. (14), the total deformation of whole stack, Z_{total}^F , can be obtained:

$$Z_{\text{total}}^F = -(MZ_{\text{initial}}^F) + Z_{\text{stack}}^F = -(MZ_{\text{initial}}^F) - \frac{Ck_{\text{bolt}}}{Ck_{\text{bolt}} + k_{\text{stack}}} \delta_{\text{fasten}} \quad (22)$$

where Z_{stack}^F denotes the whole stack deformation after the gap vanishes. Here the clamping load applied on the stack structure is:

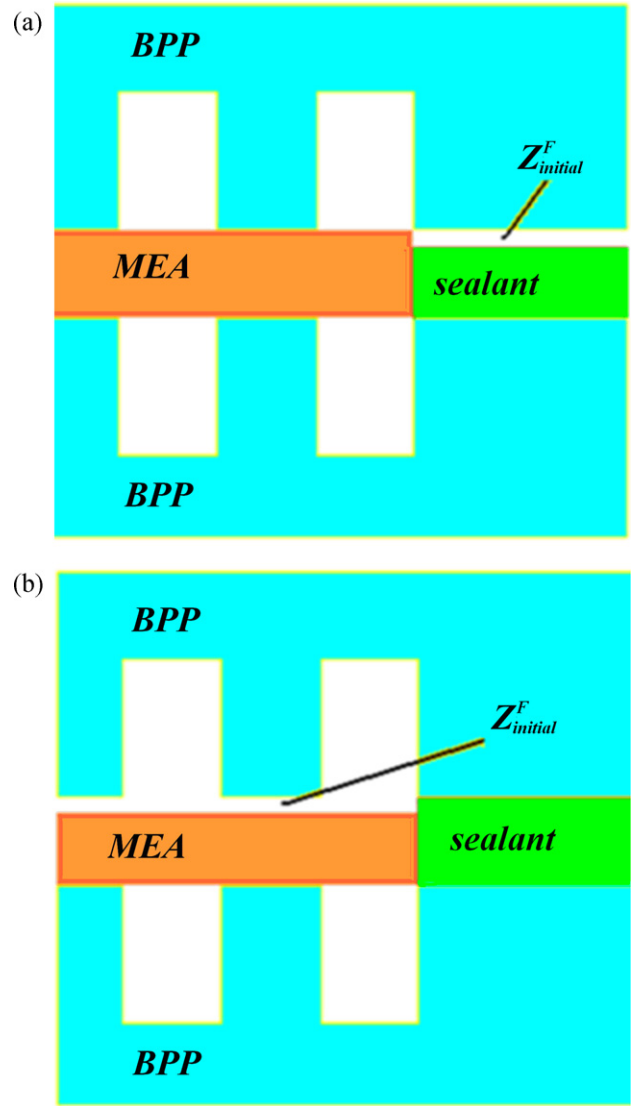


Fig. 8. Schematic of unequal thickness of the MEA and sealant before assembly: (a) a gap exists at the interface of the sealant and BPP; (b) a gap exists at the interface of the MEA and BPP.

$$\begin{aligned} F_{\text{internal-stack}} &= k_{\text{internal-stack}} Z_{\text{total}}^F \\ &= -k_{\text{internal-stack}} \left(MZ_{\text{initial}}^F + \frac{Ck_{\text{bolt}}}{Ck_{\text{bolt}} + k_{\text{stack}}} \delta_{\text{fasten}} \right) \end{aligned} \quad (23)$$

$$F_{\text{external-stack}} = k_{\text{external-stack}} Z_{\text{stack}}^F = -\frac{Ck_{\text{bolt}}k_{\text{external-stack}}}{Ck_{\text{bolt}} + k_{\text{stack}}} \delta_{\text{fasten}} \quad (24)$$

In the case of $L_{\text{MEA}} > L_{\text{sealant}}$, we have (see Fig. 8b):

$$\delta_{\text{initial}} = -\frac{MZ_{\text{initial}}^F(Ck_{\text{bolt}} + k_{\text{external-stack}})}{Ck_{\text{bolt}}} \quad (25)$$

and the total deformation of the whole stack is:

$$Z_{\text{total}}^F = MZ_{\text{initial}}^F - \frac{Ck_{\text{bolt}}}{Ck_{\text{bolt}} + k_{\text{stack}}} \delta_{\text{fasten}} \quad (26)$$

Also the clamping loads applied on the stack are:

$$F_{\text{internal-stack}} = k_{\text{internal-stack}} Z_{\text{stack}}^F = -\frac{Ck_{\text{bolt}}k_{\text{internal-stack}}}{Ck_{\text{bolt}} + k_{\text{stack}}} \delta_{\text{fasten}} \quad (27)$$

$$F_{\text{external-stack}} = k_{\text{external-stack}} Z_{\text{total}}^F$$

$$= k_{\text{external-stack}} \left(MZ_{\text{initial}}^F - \frac{Ck_{\text{bolt}}}{Ck_{\text{bolt}} + k_{\text{stack}}} \delta_{\text{fasten}} \right) \quad (28)$$

2.4.2. Effect of temperature

Temperature variation can cause thermal deformation. For the structure shown in Fig. 1, when the temperature is changed by ΔT , the free axial thermal deformation will be:

$$\Delta L = \alpha \Delta T L \quad (29)$$

If this deformation is partially or fully constrained, the thermal stress will be generated inside the fuel cell structures. As shown in Fig. 9, the thermal deformation of the whole fuel cell stack can be obtained based on the compatible displacement and static load equilibrium conditions:

$$Z_{\text{stack}}^T = \frac{Ck_{\text{bolt}}Z_{\text{bolt}}^T + k_{\text{internal-stack}}Z_{\text{internal-stack}}^T + k_{\text{external-stack}}Z_{\text{external-stack}}^T}{Ck_{\text{bolt}} + k_{\text{internal-stack}} + k_{\text{external-stack}}} \quad (30)$$

According to Eqs. (15) and (16) the combined loads applied on the stack are:

$$F_{\text{internal-stack}} = k_{\text{internal-stack}} Z_{\text{stack}}^F + k_{\text{internal-stack}} (-Z_{\text{internal-stack}}^T + Z_{\text{stack}}^T) \quad (31)$$

$$F_{\text{external-stack}} = k_{\text{external-stack}} Z_{\text{stack}}^F + k_{\text{external-stack}} (-Z_{\text{external-stack}}^T + Z_{\text{stack}}^T) \quad (32)$$

where the free thermal deformation of the internal-stack and the external-stack can be given using the equivalent clamping stiffness

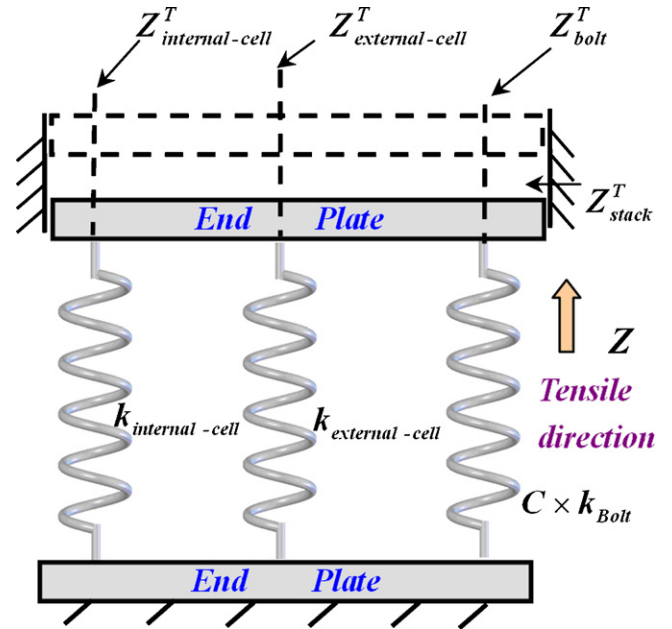


Fig. 9. Schematic of the equivalent stiffness model of the PEM stack when considering the thermal effect.

model shown in Fig. 7:

$$Z_{\text{internal-stack}}^T = \sum_{i=1}^{M+1} (Z_{\text{BPP-base}}^{T(i)}) + \sum_{j=1}^M (Z_{\text{cell-core}}^{T(j)}) \quad (33)$$

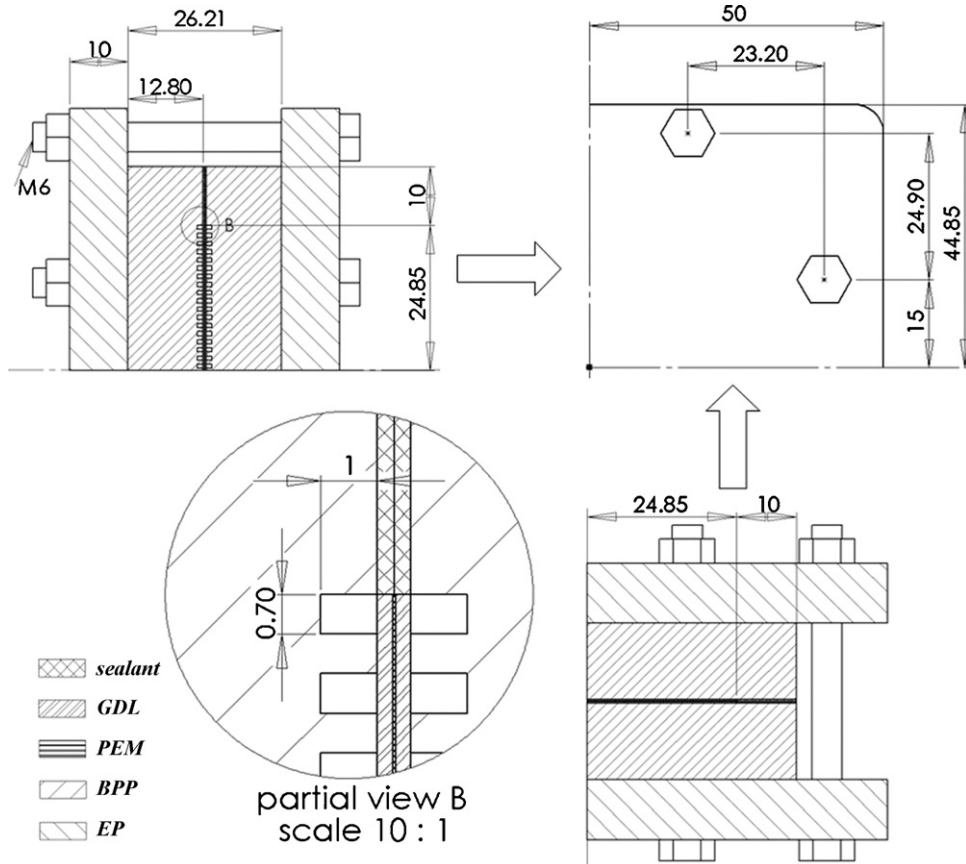


Fig. 10. Dimensions of the single cell model.

$$Z_{\text{external-stack}}^T = \sum_{i=1}^{M+1} \left(Z_{\text{BPP-sealant}}^{T(i)} \right) + \sum_{j=1}^M \left(Z_{\text{sealant}}^{T(j)} \right) \quad (34)$$

In addition, the thermal deformations of the basic components can be calculated referring to Table 1. Therefore the thermal deformations of the assembled components are obtained based on the thermal deformations of the basic components (see Fig. 4).

2.5. Determination of the assembly parameters using the equivalent stiffness model

Systematical use of the equivalent stiffness model can form a high efficient assembly technique for fuel cell stacks.

- (1) After obtaining the basic information such as component dimensions and material properties, the equivalent clamping stiffness of the basic components and assembled components can be calculated using the method mentioned above.
- (2) Based on the obtained stiffness, the clamping load of the stack and the contact pressures on the important interfaces are calculated. Thus the internal stress of the components can be calculated and the contact electrical resistance can be obtained using the equations given in refs. [1–3].
- (3) The range of the clamping load can be determined. For the lower bound, the clamping load should be large enough to provide reasonable contact pressures for the contact electrical resistance and the sealing pressure. For the upper bound, the clamping load should not be so large that the internal stress of the basic components reaches the yield stress. Finally the optimal clamping load can be determined and other clamping parameters such as the stiffness and strength of the clamping bolts can be designed in the same way.

3. Comparisons of the model analysis and FEA analysis

In order to verify the equivalent stiffness model, comparisons of the model analysis and the accurate analysis using FEA have been carried out based on the PEM single cell described in refs. [5,19–21]. The commercial FEA code of MSC. Marc was used in this study.

3.1. FEA model definition

3.1.1. Geometry

Based on the two-dimensional (2 D) FEA model proposed in refs. [5,19–21], a three-dimensional (3 D) FEA model is established. It is 1/8 of a single cell due to the structural symmetry. The present 3 D model consists of the bipolar plate, the GDL, the PEM and the sealant, while the end-plates and the clamping bolts are not considered in the numerical analysis. Dimensions of the PEM single cell can be obtained from Fig. 10, other parameters not defined in the figure are: the number of the ribs (35), the thickness of the PEM (0.05 mm), the thickness of the GDL (0.275 mm), and the thickness of the sealant (0.3 mm). Here the MEA and sealant have the same thickness.

3.1.2. Mesh and mechanical properties

Mapped meshing is adopted in order to ensure proper element connectivity and reasonable aspect ratio. The complete mesh includes 240,211 nodes and 195,516 elements (see Fig. 11a). Full integration hexahedron elements (element 7) have been used. Mechanical properties of each component are listed in Table 2. All the components are assumed to have linear elastic behavior.

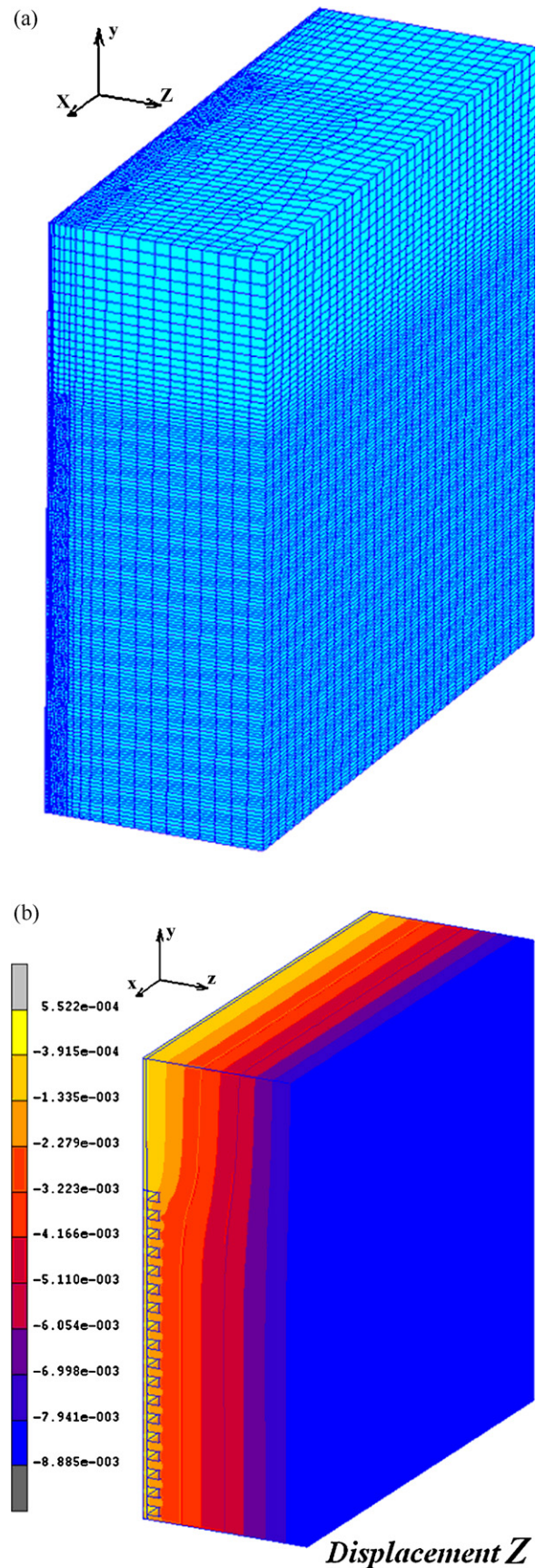


Fig. 11. Three-dimensional contact model: (a) mesh and (b) contour plot of the deformation along the clamping direction (z-axis).

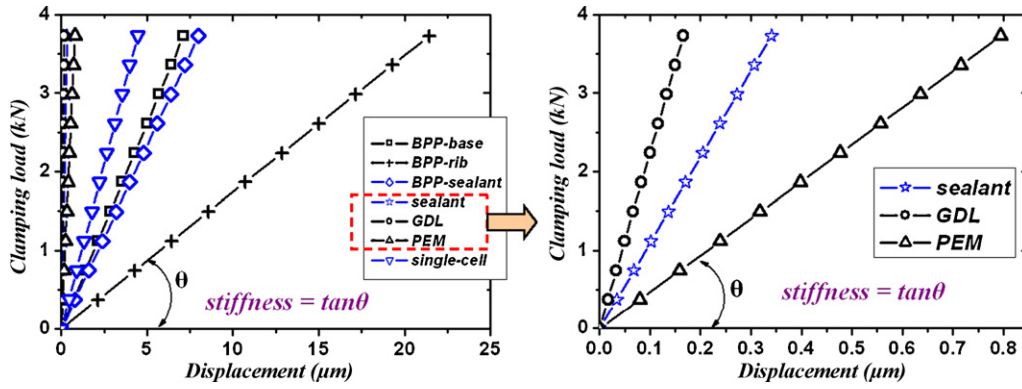


Fig. 12. Relations between the load and the displacements of the single cell structures.

3.1.3. Boundary conditions

Symmetry constraints are set on the symmetrical planes in order to prevent free movements. The efficient contact algorithm of MSC. Marc is used to compute the interactions between the components. In addition, the end-plate is replaced by a rigid surface controlled by the control node [22]. The clamping load increasing linearly from 0 to 1865 N per bolt [5] is directly applied on the control node to give a uniform pressure on the bipolar plate.

3.2. Simulation results and comparisons

Fig. 11b shows that under the uniform pressure, all the components deform nearly uniformly along the clamping direction according to the well-layered contour plot. The contour lines only fluctuate slightly at structural junctions especially for the bipolar plate consisting of BPP-base, BPP-rib and BPP-sealant. This phenomenon strongly supports the initial assumption (4). Using the control node, displacement of the single cell structure can be obtained. In the same way, a load deformation diagram of the 1/8 single cell structure is given in Fig. 12. It shows that both the single cell and its components deform almost linearly with the displacement. Therefore the corresponding equivalent stiffness can be obtained by calculating the slopes of the curves.

Meanwhile, the corresponding equivalent stiffness of the components can be calculated using the equations mentioned above and those given in Table 1. In addition, the two layers of sealants of the single cell can be combined in series as a whole in the model analysis (MA). Thus, for the same structure, the MA is compared with the FEA in Table 3. The relative error using the model analysis is

$$\text{Error} = \frac{\text{abs}(\text{MA} - \text{FEA})}{\text{FEA}} \times 100\% \tag{35}$$

Table 2
Material properties of the single cell hardware.

Property	Value	Source
PEM (Nafion®)		
Young's modulus (E) (MPa)	90 (300 K, 35% humidity)	[19]
Poisson's ratio (μ)	0.25	[19]
GDL (carbon paper)		
Young's modulus (E) (GPa)	10	[19]
Poisson's ratio (μ)	0.25	[19]
Bipolar plate (BPP)		
Young's modulus (E) (GPa)	10	[19]
Poisson's ratio (μ)	0.25	[19]
Sealant (VMQ)		
Young's modulus (E) (MPa)	5500	[4]
Poisson's ratio (μ)	0.3	[4]

Table 3
Result comparisons of the MA and the FEA.

Components	Equivalent stiffness ($\times 10^6 \text{ N mm}^{-1}$) MA	Equivalent stiffness ($\times 10^6 \text{ N mm}^{-1}$) FEA	Relative error
BPP-base (1/4)*	0.523324	0.523325	<1
BPP-rib (1/2)	0.17395	0.17395	<1
BPP-sealant (1/4)	0.466406	0.46641	<1
Sealant (1/4)	10.945	10.945	<1
GDL (1/4)	22.45536	22.45534	<1
PEM (1/8)	4.69316	4.69318	<1
Single cell (1/8)	0.84783	0.83961	<3

* Values in the brackets in column 1 indicate the symmetry of the basic components and the single cell structure.

Table 3 shows that the results calculated by the two methods are very close. The relative error for the basic component is less than 1%, and even for the whole single cell structure the relative error is no more than 3%. In addition, it costs nearly 10 h for the FEA to obtain the results on a high performance hardware platform with 4 cores CPU and 4 GB memory; while it costs about 15 min by hand calculation and it may need only a few seconds using the computer programming based on this model analysis. All the calculations mentioned above show that the equivalent stiffness model has a highly efficiency and gives a very good prediction accuracy.

4. Discussions and conclusions

The clamping load applied on the fuel cell stack should be fit for the corresponding structures since the mechanical behavior of the fuel cell stack has a profound affect on the fuel cell performance. Too high a clamping load will not only reduce the permeability of the GDL and then reduce the power density of the fuel cell stack, but also may cause some components in the stack to produce a high stress as a result that a plastic deformation even crack may take place; However, an unreasonably low clamping load may cause a high contact electrical resistance at the interface of the GDL and the BPP, and a leakage of either water or fuel in the seal interfaces [1–3]. Moreover, even though the average stress in a component is lower than the yield stress, a fatigue failure may occur during the running time of the stack if the stress variation range due to either the temperature or other working conditions is considerably large.

In this paper, a large fuel cell stack has been simplified to an equivalent stiffness model consisting of numerous elastic elements (springs) in parallel or series connections. Starting with a single PEM fuel cell, an equivalent stiffness model of the whole fuel cell stack is developed. Then the effects of the temperature and structure parameters on the internal stress, contact resistance and the sealing pressure of the components are discussed. Finally, a high efficient assembly technique for a large PEMFC stack using the equivalent stiffness model has been proposed. With this technique,

a reasonable clamping load and optimal stiffness of the related components for a large fuel cell stack can be obtained.

Comparisons of the model analysis and the accurate analysis using FEA have been carried out based on a typical PEM single cell. A numerical analysis using a three-dimensional nonlinear contact model shows that the prediction error of the stiffness for each component of a single fuel cell using the present model is less than 1%, and even for the whole single cell structure the relative error is no more than 3%.

In the present part of the study for the assembly technique of a large fuel cell stack, we used a rigid end-plate assumption. This may causes some error for the structure design and the prediction of the internal stress and the interface contact pressure of the fuel cell components, especially for the cells near the end-plates. However, if the end-plate is so specially designed that the interfaces of the components inside the stack can be kept as an approximate plane, the rigid end-plate assumption is still valid. The work how to modify the present assembly model for an elastic end-plate and how to use the present model to design the structures for a large fuel cell stack is being done in the present research group and will be published in additional paper.

Acknowledgements

This work was supported by the National Natural Science Foundation of China (10672035, 10721062, 90816025) and “863” project 2007AA04Z405.

References

- [1] P. Zhou, C.W. Wu, G.J. Ma, J. Power Sources 159 (2006) 1115–1122.
- [2] P. Zhou, C.W. Wu, G.J. Ma, J. Power Sources 163 (2007) 874–881.
- [3] P. Zhou, C.W. Wu, J. Power Sources 170 (2007) 93–100.
- [4] S.J. Lee, C.D. Hsu, C.H. Huang, J. Power Sources 145 (2005) 353–361.
- [5] D. Bograchev, M. Gueguen, J.C. Grandidier, S. Martemianov, J. Power Sources 180 (2008) 393–401.
- [6] X.M. Lai, D.A. Liu, L.F. Peng, J. Ni, J. Power Sources 182 (2008) 153–159.
- [7] Z.Y. Su, C.T. Liu, H.P. Chang, C.H. Li, K.J. Huang, P.C. Sui, J. Power Sources 183 (2008) 182–192.
- [8] K. Hertwig, L. Martens, R. Karwoth, Fuel Cells 2 (2003) 61–77.
- [9] J. Gou, P.C. Pei, Y. Wang, J. Power Sources 162 (2006) 1104–1114.
- [10] K. Chu, J. Ryu, M. Sunwoo, J. Power Sources 171 (2007) 412–423.
- [11] S. Kamarajugadda, S. Mazumder, J. Power Sources 183 (2008) 629–642.
- [12] D.H. Ahmed, H.J. Sung, J. Bae, Int. J. Hydrogen Energy 33 (2008) 3786–3800.
- [13] A. Bazylak, D. Sinton, Z.S. Liu, N. Djilali, J. Power Sources 163 (2007) 784–792.
- [14] S.P. Timoshenko, J.N. Goodier, Theory of Elasticity, Second ed., McGraw-Hill, New York, 1951.
- [15] A. Bouzidane, M. Thomas, Tribol. Transactions 50 (2007) 257–267.
- [16] J.S. Kim, J.B. Park, Y.M. Kim, et al., Int. J. Precision Eng. Manuf. 9 (2008) 39–46.
- [17] V. Mehta, J.S. Cooper, J. Power Sources 114 (2003) 32–53.
- [18] F.A. de Bruijn, V.A.T. Dam, G.J.M. Janssen, Fuel Cells 8 (2008) 3–22.
- [19] A. Kusoglu, A.M. Karlsson, M.H. Santare, S. Cleghorn, W.B. Johnson, J. Power Sources 161 (2006) 987–996.
- [20] Y. Tang, M.H. Santare, A.M. Karlsson, S. Cleghorn, W.B. Johnson, J. Fuel Cell Sci. Technol. 3 (2006) 119–124.
- [21] A. Kusoglu, A.M. Karlsson, M.H. Santare, S. Cleghorn, B.J. William, J. Power Sources 170 (2007) 345–358.
- [22] Marc2007r1 Volume E: Demonstration Problems, MSC software, 2007.